Velocity of Transverse Domain Wall Motion Along Thin, Narrow Strips

D. G. Porter, M. J. Donahue

National Institute of Standards and Technology,

Gaithersburg, MD 20899

Abstract— **Micromagnetic simulation of domain wall motion in thin, narrow strips leads to a simplified analytical model. The model accurately predicts the same domain wall velocity as full micromagnetic calculations, including dependence on strip width, thickness, and magnitude of applied field pulse. Domain wall momentum and retrograde domain wall motion are both observed and explained by the analytical model.**

Fig. 1. Transverse domain wall in thin, narrow strip.

I. Introduction

The effects of the shape and small dimensions on magnetodynamics are important so that devices can be produced to meet magnetization reversal design requirements. In this study we first use micromagnetic simulation to examine domain wall motion in thin, narrow strips of magnetic material. Inspired by the simulation results, we then produce a simpler analytical model that agrees with the full micromagnetic simulation remarkably well. Both models predict a few unexpected behaviors.

II. Simulation

Using the OOMMF micromagnetic software package [1], we examined domain wall motion in a strip $T = 5$ nm thick and $L = 1250$ nm long. Our simulations included strips of width W ranging from 5 nm to 35 nm. Material parameters approximating Permalloy were chosen, with saturation magnetization $M_S = 800$ kA/m and exchange energy coefficient $A = 13$ pJ/m. Crystalline anisotropy was not included in the simulation of this soft material. Landau-Lifshitz magnetization dynamics are computed:

$$\frac{dm}{dt} = \frac{\gamma}{1+\alpha^2} m \times H_{\text{eff}} - \frac{\alpha\gamma}{1+\alpha^2} m \times H_{\text{eff}} \times m, \quad (1)$$

where $\gamma = -221$ kHz/(A/m) is the gyromagnetic constant, α is a dimensionless phenomenological damping parameter, $m = M/M_S$ is normalized magnetization, and H_{eff} is the effective field representing the effect of all energies included in the simulation.

From a prior simulation study [2] of static domain walls in thin, narrow strips, we expect head-to-head domains to be separated by a transverse domain wall as illustrated in Fig. 1. We have used the same technique as in that prior study to suppress edge effects, to focus on the behavior of a domain wall down the length of a strip, far removed from the ends.

The initial transverse domain wall is established in the element. A field pulse is applied along the strip axis,

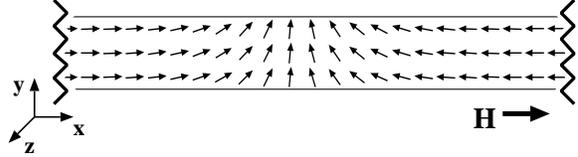$$\mu_0 H_x(t) = \mu_0 H_{\text{app}}(1 - \cos 2\pi f t), \ 0 < t < 1 \text{ ns} \quad (2)$$

where $f = 1$ GHz, so that the 1 ns pulse includes one full cosine period. Pulse magnitudes $\mu_0 H_{\text{app}}$ from 1 to 10 mT were applied. In response to each applied field pulse, the transverse domain wall moves in the positive x direction. After the pulse ends, the domain wall continues to move with a momentum of its own. Simulations with $\alpha = 0$ demonstrate that the domain wall motion is primarily a precessional effect.

Because the transverse domain wall holds its shape and the domains remain uniformly magnetized along the strip axis, the wall velocity can be derived from the average magnetization of the whole element,

$$v(t) = \frac{L}{2} \frac{d < m_x(t) >}{dt}. \quad (3)$$

When $\alpha = 0$, the domain wall momentum moves the wall at constant velocity. When $\alpha > 0$, the domain wall stops some time after the pulse ends, although for large enough applied field pulses, the wall velocity increases after the pulse ends before slowing to a stop.

Figure 2 graphs constant wall velocities observed when $\alpha = 0$ for several values of strip width W and pulse magnitude $\mu_0 H_{\text{app}}$. For each W, there is a pulse magnitude that maximizes wall velocity. For wider strips, a lesser pulse magnitude produces the maximum velocity and that maximum velocity is greater.

Another set of simulations applied a constant field rather than a pulse. The remarkable observation was that for large enough applied field, the domain wall velocity becomes negative part of the time, leading to a retrograde motion of the domain wall.

III. Domain Wall Structure

As a first step toward deriving an analytical model to explain these simulation results, we examine the structure of the domain wall itself. First we note that within the scales under study, the magnetization can be considered to vary along only the x axis, $M(x, y, z) = M(x)$.
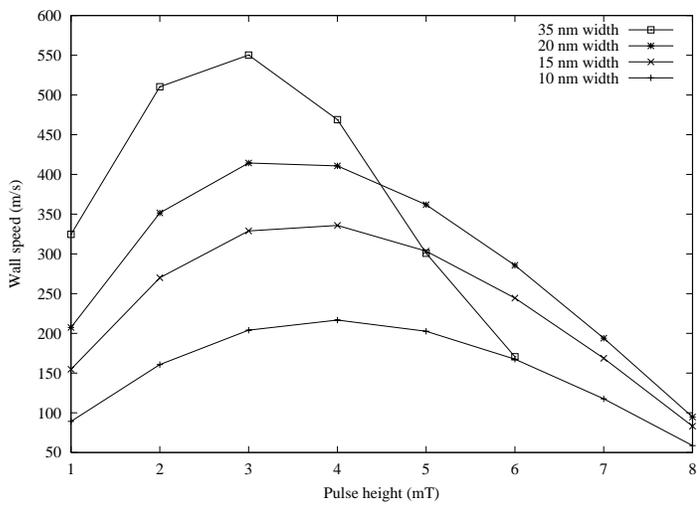
Fig. 2. Domain wall velocity for various strip widths and applied field pulse magnitudes

Exchange energy prefers to spread the wall along the entire length of the strip. The shape anisotropy of the strip, however, tends to expand the domains at the expense of the wall. The actual width of the domain wall comes from a balancing of these two energies, in a manner precisely analogous to the well-known one-dimensional domain wall model where exchange and crystalline anisotropy energies are balanced.

Most of the shape anisotropy energy comes from surface charges due to the transverse components of magnetization. As an approximation, we neglect the magnetostatic energy from bulk charges, and compute the demagnetization energy of an in-plane transverse wall as

$$E = -\frac{\mu_0 M_S}{2} \int_V m_y(x) H_y(x,y,z) dx\,dy\,dz, \qquad (4)$$

where $H_y(x)$ arising from the surface charges is

$$H_y(x,y,z) \quad = \int_0^L \int_0^T m_y(x') \quad M_S\{f(x-x',y-W,z-z') \\ -f(x-x',y,z-z')\}dz'dx',$$

where

$$f(x,y,z) = \frac{y}{[x^2+y^2+z^2]^{\frac{3}{2}}}. \qquad (5)$$

After rearrangement and simplification

$$E = \frac{\mu_0 M_S^2}{2} \int_0^L \int_0^L m_y(x) m_y(x') \Phi(x-x') dx\,dx', \qquad (6)$$

where Φ is integrable and has most weight near zero, so acts approximately as a Dirac delta function. Following the same calculus of variations analysis as for crystalline anisotropy energy,

$$E = K_y \int_0^L m_y^2(x) dx, \qquad (7)$$

leads to the expression for an effective shape anisotropy constant for a given strip width W and thickness T,

$$K_y(W,T) = \frac{\mu_0 M_S^2}{2}\{1 - \frac{2}{\pi}\tan^{-1}(\frac{W}{T}) \qquad (8)$$

$$+ \quad \frac{1}{2\pi}\frac{T}{W}\log(1+(\frac{W}{T})^2) - \frac{1}{2\pi}\frac{W}{T}\log(1+(\frac{T}{W})^2)\}.$$

By an analogous argument, the shape anisotropy constant for a domain wall directed out of the plane in the z direction is

$$K_z(W,T) = K_y(T,W). \qquad (9)$$

Following the classical analysis of one-dimensional models of domain walls, this approximation predicts the width of a domain wall tilted at angle θ out of the plane to be

$$a = \pi\sqrt{\frac{A}{K_y \cos^2\theta + K_z \sin^2\theta}}. \qquad (10)$$

From the simulations, we can compute a different estimate of the domain wall width of the magnetization state,

$$\hat{a} = L(<m_y>^2 + <m_z>^2)^{\frac{1}{2}}. \qquad (11)$$

The $\hat{a}$ estimate from simulations are consistently slightly larger (10 - 20 %) than the predicted value a, presumably due to the neglected bulk charges. To compensate for this difference, in the remainder of the paper we use a value of a that is 15% greater than the value predicted by (10).

IV. ANALYTICAL MODEL

Consider a partition of the strip into three regions: the two domains, each uniformly magnetized, and the domain wall uniformly magnetized in the transverse direction over a length a of the strip. The domains are magnetized parallel to the applied field, so they do not respond to it . The domain wall region does respond. Damping toward the applied field causes the domain wall to rotate toward the positive x axis. Precession about the applied field causes the domain wall magnetization to tilt out of the plane at an angle θ. After the magnetization tilts out of plane, it is no longer anti-parallel to the demagnetization field. The component of demagnetization field perpendicular to the magnetization, $H_D^\perp$, is

$$H_D^\perp = M_S(N_z - N_y)\cos\theta\sin\theta, \qquad (12)$$

where N_y and N_z are the demagnetizing factors of the $a \times W \times T$ region containing the domain wall [3]. For non-zero θ, $H_D^\perp$ is also non-zero, and the domain wall magnetization will precess around it, contributing to the rotation toward the positive x axis. The complete expression for velocity of the domain wall predicted by this simple model is

$$(1 + \alpha^2)v = (|\gamma|/\pi)(H_D^\perp + \alpha H_{app})a. \qquad (13)$$

After H_{app} returns to zero, the precession about the demagnetizing field sustains the momentum of the domain wall. This phenomenon is completely analogous to the momentum predicted by a 1D model of a Bloch wall [4]. Damping will slowly draw energy from the system, and eventually bring the domain wall to a stop.

It is clear from these expressions that for any particular strip geometry, there is a tilt angle θ that maximizes

domain wall velocity. The time rate of change of the tilt angle is

$$(1 + \alpha^2)\frac{d\theta}{dt} = |\gamma|(H_{\text{app}} - \alpha H_D^\perp). \qquad (14)$$

For the applied field pulses, the total tilt angle θ achieved by the end of the pulse is proportional to the area under the applied field pulse. It is also clear that larger velocities are expected as $(N_z - N_y)$ grows larger; that is, as the width-to-thickness ratio of the strip increases. These relationships explain the features of the micromagnetic simulation results in Fig. 2. When the applied field pulse creates a tilt angle θ greater than that which maximizes velocity, the model predicts that after the pulse, as damping decreases θ, the wall velocity will actually increase before it decreases and the wall comes to a stop, just as observed in micromagnetic simulation.

This analytical model can also explain the response of domain walls to a constant applied field. When the applied field is small enough, its tendency to increase the tilt angle θ will eventually be exactly balanced by the tendency of the damping to push θ back to zero. Specifically, for $H_{\text{app}} < \alpha \max_\theta H_D^\perp$, a constant θ is reached and the wall moves at the constant velocity determined by that tilt angle.

For larger H_{app}, θ will continue to grow as precession about the applied field continues past the z axis ($\theta = \pi/2$). Once θ exceeds $\pi/2$, both precession and damping combine to accelerate the magnetization back into the plane. Though precession continues clockwise around $H_D^\perp$, the transverse direction of magnetization is reversed, so that precession moves the wall in the reverse direction. That is, the domain wall velocity becomes negative. As θ exceeds π, the magnetization passes through the plane of the strip, and the direction of $H_D^\perp$ is reversed, causing the precession direction to reverse, yielding another reversal of wall direction. The same pattern repeats as the precession about the applied field continues for $\pi < \theta < 2\pi$. The number of cycles of domain wall direction reversal is exactly twice the number of precession rotations about the applied field.

For $H_{\text{app}} > \alpha^{-1} \max_\theta H_D^\perp$, we know from (13) that wall velocity will not be negative, so for such large fields retrograde motion will cease, though the domain wall tilt angle θ will continue to precess around the strip axis.

Figure 3 depicts how well the simple analytical model succeeds in predicting the same domain wall position as a function of time as a full micromagnetic calculation. The solid line is the wall trajectory predicted by numeric integration of (13). Wall width a ranges from 24 to 39 nm during each precession cycle. Figure 4 is a direct illustration of the retrograde motion of the domain wall in the presence of a constant applied field.

Equations (12) - (14) are substantially similar to those derived in a previous study of domain wall dynamics in nanowires [5]. However, in our work, we have derived the dependence of $H_D^\perp$ on W, T, and θ, while the previous work assumed a simple uniaxial anisotropy form of the demagnetization energy. If we made the same assumptions, our threshold for observing retrograde domain wall motion would be $H_{\text{app}} < \alpha M_S (N_z - N_y)/2$ which corresponds to
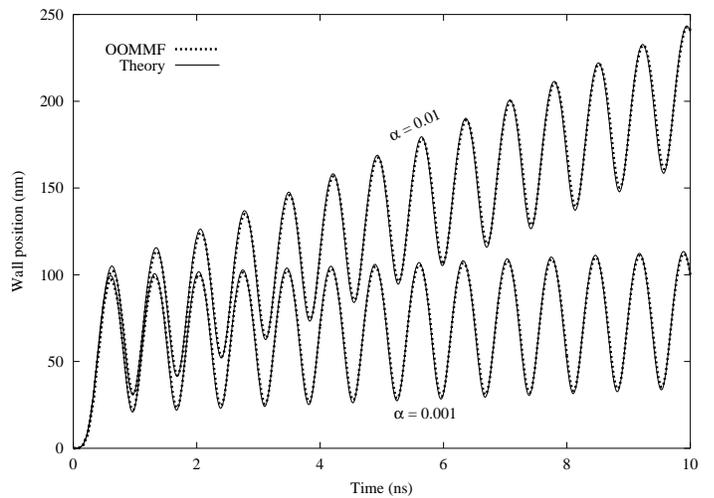

Fig. 3. Comparison of the predictions of the analytical model with the results computed by a full micromagnetic simulation. Response of a transverse domain wall to an applied field ramped up to a constant value. $\mu_0 H_{\text{app}} = 25$ mT, $W = 15$ nm, $\alpha = 0.001$ and $\alpha = 0.01$.
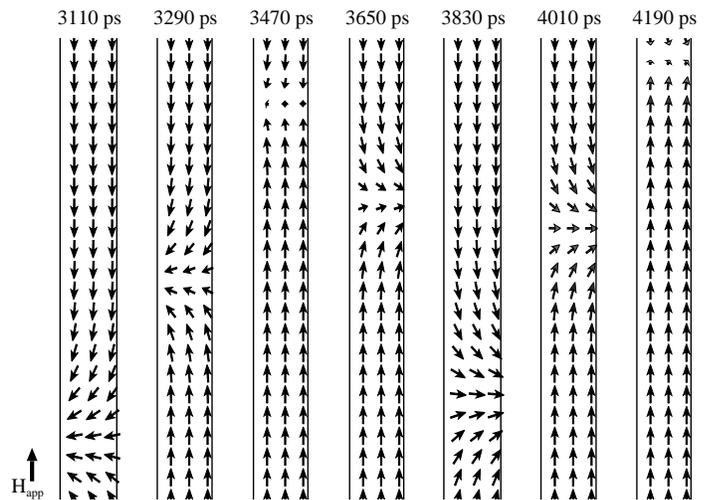

Fig. 4. A sequence of magnetization patterns, illustrating retrograde domain wall motion driven by a constant applied field. At 3470 ps the wall is tilted up. At 4190 ps the wall is tilted down.

the "Walker field" predicted by the earlier work. It should be noted that although the analytical work in Ref. 5 is sound, the simulation results reported are invalid because the demagnetization fields are computed using a sampling technique rather than an averaging technique, a simulation error we have fully described elsewhere [6].

REFERENCES

[1] Michael J. Donahue and Donald Gene Porter, NISTIR 6376, National Institute of Standards and Technology, 100 Bureau Drive, Gaithersburg, MD 20899, 1999.
[2] Robert D. McMichael and Michael J. Donahue, *IEEE Trans. Magn.*, vol. 33, pp. 4167–4169, 1997.
[3] Andrew J. Newell, Wyn Williams, and David J. Dunlop, *Journal of Geophysical Research - Solid Earth*, vol. 98, no. B6, pp. 9551–9555, June 1993.
[4] Sushin Chikazumi, *Physics of Magnetism*, p. 348, Robert E. Krieger Publishing Company, 1964.
[5] A. Thiaville, J. M. García, and J. Miltat, *Journal of Magnetism and Magnetic Materials*, vol. 242, pp. 1061–1063, 2002.
[6] M. J. Donahue, D. G. Porter, R. D. McMichael, and J. Eicke, *J. Appl. Phys.*, vol. 87, no. 8, pp. 5520–5522, April 2000.